Cellular automata models of single-lane traffic

Márton Sasvári[1,2] and János Kertész[2]
[1]*Institute of Physics, Eötvös University, H-1088 Puskin u. 5-7, Hungary*
[2]*Department of Theoretical Physics, Technical University of Budapest, Budafoki út 8, H-1111, Hungary*
(Received 5 May 1997; revised manuscript received 16 July 1997)

The jamming transition in the stochastic cellular automation model (Nagel-Schreckenberg model [J. Phys. (France) I **2**, 2221 (1992)]) of highway traffic is analyzed in detail by studying the relaxation time, a mapping to surface growth problems, and the investigation of correlation functions. Three different classes of behavior can be distinguished depending on the speed limit $v_{\max}$. For $v_{\max}=1$ the model is closely related to the Kardar-Parisi-Zhang class of surface growth. For $1<v_{\max}<\infty$ the relaxation time has a well-defined peak at a density of cars ρ somewhat lower than the position of the maximum in the fundamental diagram: This density can be identified with the jamming point. At the jamming point the properties of the correlations also change significantly. In the $v_{\max}=\infty$ limit the model undergoes a first-order transition at $\rho\to 0$. It seems that in the relevant cases $1<v_{\max}<\infty$ the jamming transition is under the influence of a second-order phase transition in the deterministic model and a first-order transition for $v_{\max}=\infty$. [S1063-651X(97)10810-8]

PACS number(s): 05.40.+j

I. INTRODUCTION

The breakthrough in statistical physics due to the understanding of critical phenomena and the related development of methods has initiated vivid interdisciplinary research activity. The successful application of these methods demonstrates that the validity of the concepts to handle the problem of many interacting units reaches far beyond the traditional scope of statistical physics.

Vehicular traffic represents, from the point of view of statistical physics, a far-from-equilibrium driven system where a combination of the highway code and individual driving strategies replaces the usual physical interactions between particles. Of course, the approach of a physicist is quite different from that of a traffic engineer: We would like to model the typical behavior as simply as possible while the essence of some phenomena should remain unaltered, though it is not our aim to describe specific traffic situations. Nevertheless, one can hope for a twofold gain from these type of studies: First, they could help us to understand far-from-equilibrium systems and, second, we strongly believe that the concepts developed in physics can contribute to the understanding of the complex phenomena related to vehicular traffic. Obvious analogies to problems of physics such as kinetic theory or granular flow have motivated physicists to work in this field. In fact, natural scientists' contributions to the understanding of traffic problems already have a long history [1,2].

Numerous articles have been published in the past few of years investigating discrete models of highway traffic flow [3–7]. It was suggested that very simple probabilistic models based on cellular automata can reproduce features of real traffic, including a supposed transition from low-density laminar flow to a high-density phase, where start-stop waves are dominant. The behavior of these simple models is very complex near this transition and up to now is still not well understood.

The paper is organized as follows. In the next section we summarize the model and the method of simulation. In Sec. III the relaxation-time analysis is presented. Section IV deals with the relation of traffic models to surface growth. The correlation functions are analyzed in Sec. V. The special case of no speed limit is discussed in Sec. VI. The paper concludes in Sec. VII.

II. MODEL AND SIMULATION

In this paper we consider the cellular automata introduced by Nagel and Schreckenberg to describe single-lane traffic [3]. The model consists of a one-dimensional array of L cells with periodic boundary conditions. Every cell has $v_{\max}+2$ states: It can be empty or it can contain a car with velocity $v=0,1,...,v_{\max}$. The density of cars is ρ. We perform the following steps in parallel for all cars: (a) acceleration, increase v by 1 if possible; (b) deceleration, decrease v to avoid a crash with the car in front, (c) randomization, decrease v by 1 with probability p if possible, and (d) movement, move forward v sites.

Despite its simplicity, this model captures several aspects of highway traffic including the free-flow–jamming transition. The parameter $v_{\max}$ can be considered as a speed limit and a usual value for it is 5. We would like to stress the importance of the third step. The fact that the model uses braking noise characterized by probability p is crucial. One could equally introduce random accelerations, but it can be shown that these types of perturbations die out very quickly; see [8]. An initial condition is needed to specify the model completely.

A convenient way to investigate the model is to draw a diagram of flow versus density, the so-called *fundamental diagram*. It is a curve with a well-defined maximum at a density ρ_c. The occurrence of density waves is related to the nonlinearity of the fundamental diagram and it is expected that the jamming transition will occur somewhere near the maximum. At low densities the flow is ''free'' with very few waves due to fluctuations [step (c)] which die out quickly; at high densities above the maximum start-stop waves dominate the system, which is in the ''jammed'' state.

TABLE I. Simulations performed for the relaxation-time analysis for $v_{\max}=1$.

System size L	Number of runs
2000	10 000
4000	5000
8000	2000

What is the nature of this transition? It has been suggested [9] that, with increasing density, the jammed regions grow in space and time and at the jamming point they form a $(1+1)$-dimensional interconnected infinite network. This would point to a percolation-type picture for the process. However, the percolation transition depends on the geometry of the clusters, i.e., on the microscopic definition of jams, which introduces some ambiguity. Moreover, it was demonstrated in [10] that an appropriate choice of the parameters leads, for any reasonable jam definition, to a percolation transition at densities much higher than the region where jams become dominant. In order to resolve this problem and to avoid the ambiguity related to the definition of the jams, in [10] another definition of the jamming transition point was given without explicitly referring to the density waves. It was found that the relaxation time of the average velocity has a maximum at a well-defined density ρ_p and the value of the maximum increases with growing system sizes. This phenomenon was interpreted in [10] as a critical slowing down and the critical point in the infinite-size limit was identified with the jamming transition, which turned out to be somewhat below the density at the maximum in the fundamental diagram ($\rho_c > \rho_p$).

The interpretation of the jamming transition as a second-order nonequilibrium phase transition raises the question of the order parameter. One suggestion has been [11] to take the density of jammed cars as an order parameter that shows a rapid increase numerically at the same density where the relaxation time has its maximum. In addition to the above-mentioned problem with the definition of the jam, this ''order parameter'' has the disadvantage that, due to the random braking events, there are small jams for any nonzero car density, i.e., the order parameter would not entirely vanish even below the transition.

The present paper is devoted to a detailed investigation of the jamming transition. We have studied the model with three different values of $v_{\max}$, namely, 1, 2, and ∞. Because of the boundary conditions the $v_{\max}=\infty$ case means $v_{\max}=L$. It is widely believed that the $v_{\max}=1$ and $1<v_{\max}<\infty$ cases differ qualitatively [6] and we have found that the case without a speed limit shows interesting and unusual features. With the upper choice of the $v_{\max}$ parameters we can compare the three classes of models.

The stationary state of the $v_{\max}=1$ model is analytically exactly solvable [6]. In addition, the model has a car-hole symmetry that connects that stationary state at ρ with the stationary state at $1-\rho$. In the $v_{\max}>1$ cases this symmetry does not exist because every $v>1$ step corresponds to the common movement of several holes. Due to its relationship with other nonequilibrium models, the $v_{\max}=1$ model is not expected to exhibit a ''phase transition'' at a specific density, while this is assumed for $v_{\max}>1$.

TABLE II. Simulations performed for the relaxation-time analysis for $v_{\max}=2$.

System size L	Number of runs
2048	10 000
4096	5000
16 384	1000
32 768	500

For this reason we made simulations for the different cases and methods. We used $p=0.5$ for the braking probability throughout the paper. For the $v_{\max}=1$ and ∞ cases we used an algorithm with position and velocity coding, storing the velocities and positions of the cars in two arrays. For the $v_{\max}=2$ case we used a multispin coding algorithm where we stored the lane $v_{\max}+1$ times having L bits for every velocity according to the system size. In the lane labeled by v the ith bit is 1 when there is a car with velocity v at site i and bit zero otherwise. This algorithm is faster because we can use bitwise operations. When calculating velocity correlation functions, we used the multispin coding algorithm only for reaching the stationary state and then switched to the position coding technique that was more appropriate for the calculations afterward.

III. RELAXATION-TIME ANALYSIS

First we measured the average car velocity $\overline{v}=(1/N)\Sigma_i v_i$ as a function of time. As an initial condition we used uniformly distributed cars with $v_i=0$ for all cars and averaged over several runs. The performed simulations are listed in Tables I and II.

We used the same τ definition as introduced in [10], namely,

$$\tau=\int_0^\infty [\min(v^*(t),\langle v_\infty\rangle)-\langle\overline{v(t)}\rangle]dt, \tag{1}$$

where $v^*(t)$ is the velocity-time function of cars without interaction and v_∞ is the average velocity at the stationary state. As in [10], we found a peak in τ as a function of the density. For the $v_{\max}=2$ case τ_m, the maximum of this peak, is at $\rho_p\approx 0.15$, which is smaller than $\rho_c=0.25$ (Figs. 1 and

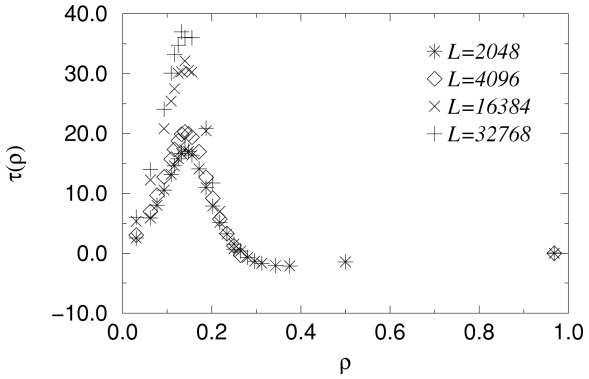

FIG. 1. Relaxation times versus density measured for the $v_{\max}=2$ case for different system sizes. The maxima of the peaks are at the density $\rho_p\approx 0.15$ and have nearly the same half-widths.

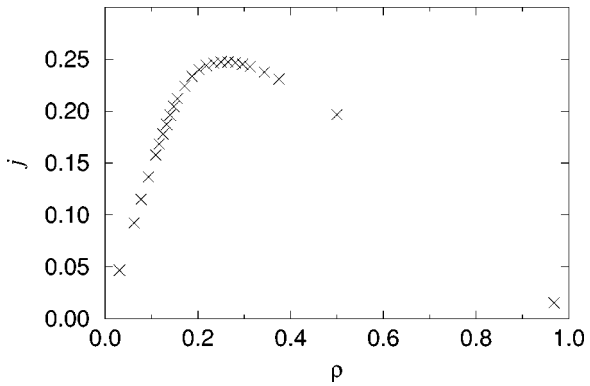

FIG. 2. Fundamental diagram for the $v_{\max}=2$ model measured for $L=2048$. The maximum of the diagram is at $\rho_c=0.25$.

2). We see in Fig. 3 that the reason for the appearance of negative relaxation times in Fig. 1 is that in this density region the average velocity function $\overline{v(t)}$ has a maximum after a fast increase for short times and it relaxes from this maximum to the stationary state. Every time step during this relaxation gives a negative contribution to τ.

Assuming that

$$\tau_m(L)\sim L^z, \tag{2}$$

we can fit $z\approx 0.286\pm 0.012$. On the other hand, $\sigma(L)$, the half-width of the τ peaks, is roughly the same. Therefore, in contrast to our earlier study with $v_{\max}=5$, we have here no implication to assume a

$$\sigma(L)\sim L^{-1/\nu} \tag{3}$$

scaling form and we could not do any finite-size scaling.

In the $v_{\max}=1$ case $\rho_c=0.5$, as is well known, and $\rho_p \approx 0.35$ (Fig. 4). The curves seem to be more similar than in the $v_{\max}=2$ case and they seem to have the same form for different system sizes. The value of the z exponent is $z=0.27\pm 0.02$. This value seems to be universal for all the $v_{\max}$ parameters taking notice of [10] too. However, in the $v_{\max}=1$ case this behavior is not bound to ρ_p, but it can be obtained in a broad range of the density.

Looking for a different definition of a relaxation time we tried to fit a

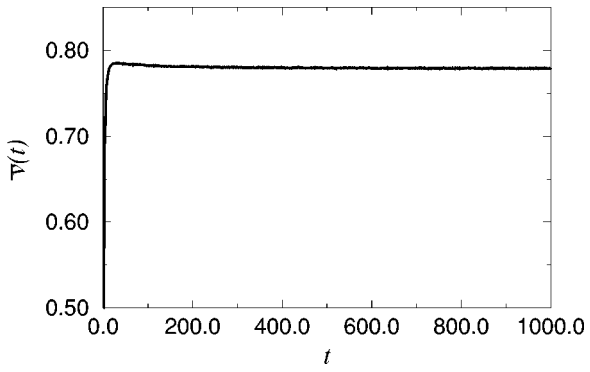

FIG. 3. Average velocity versus time graph for $v_{\max}=2$, $L=2048$, and $\rho=0.3125$.

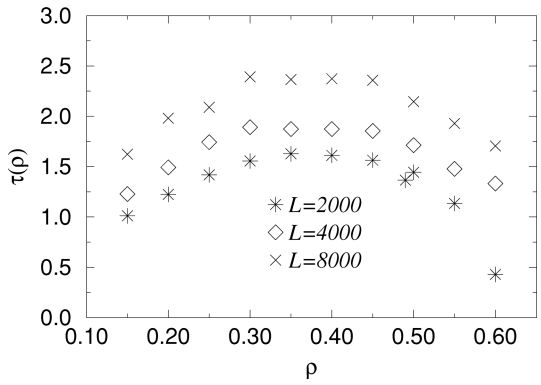

FIG. 4. Relaxation times versus density graph measured for $v_{\max}=1$. We see similar curves for different system sizes.

$$v(t)=v_\infty\left[1-bt^{-x}\exp\left(-\frac{t}{\tau}\right)\right] \tag{4}$$

function on the measured $\overline{v(t)}$ functions. Here v_∞ is the average velocity in the stationary state and b, x, and τ are fitting parameters. We began the fit after the first increasing regime, which consists of 3–10 steps, because then the car movements are nearly independent and therefore the $\overline{v(t)}$ graph is roughly a straight line.

For every fit the value of τ turned out to be larger than the corresponding system size. The exponent was vague to fit and had a great error because its effect falls in the regime of the fluctuations around $v_\infty(\rho)$, the stationary value of $\overline{v(t)}$. In the $v_{\max}=2$ case we could fit only in a restricted density region because of the shape of $\overline{v(t)}$ described above.

In the $v_{\max}=1$ case the values of the x exponent obtained were the same within errors. Their value is 0.62 ± 0.09. This value is near $\frac{2}{3}$. This value can be interpreted in terms of a mapping to the Kardar-Parisi-Zhang (KPZ) surface growth problem (see the next section).

In the $v_{\max}=2$ case the value of the x exponent increases from 0.6 to 1.5 in the measured density region (Fig. 5). We have an upper density limit for the fits because of the emerging maximum in $\overline{v(t)}$ (Fig. 3).

IV. RELATION TO SURFACE GROWTH

With an appropriate conversion, this traffic model can be transformed into a surface growth model [12]. The transfor-

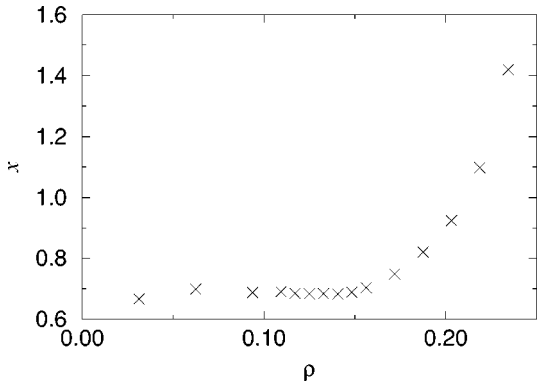

FIG. 5. x exponent versus density graph for $v_{\max}=2$.

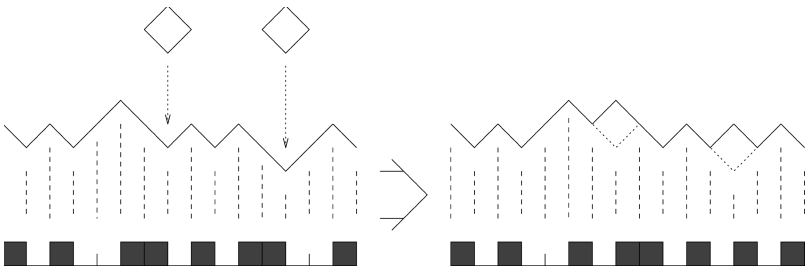

FIG. 6. Determination of the corresponding surface growth model to the traffic model.

mation is as follows. We go along the lane from left to right and order a slant line to every lattice site whose length is $\sqrt{2}$ times the lattice spacing and bevels with an angle α from the lane. At every step we order a line with a slope of $\alpha=45°$ to a car and a line with a slope of $\alpha=-45°$ to a hole. We always continue this emerging zigzag line at the end of it and we make a step upward or downward according to whether we find a hole or a car. After every update of the traffic model we get a surface in this model. The update of the traffic model determines the update of the surface growth model (Fig. 6). If the density $\rho\neq0.5$ the surface has a density-dependent average steepness of $(2\rho-1)\sqrt{2}$ because the difference of the two ends of the surface is $\sqrt{2}(2\rho-1)L$.

In the $v_{\max}=1$ case the surface growth picture corresponds to a deposition model in which we drop squares with their corner downward in every local valley with probability $1-p$ as we go from left to right. The squares have an edge of $\sqrt{2}$ times the lattice spacing. The deposition of a square corresponds to a step with velocity $v=1$ in the traffic model. This simple deposition picture does not hold for the $v_{\max}=2$ case because there are $v=2$ steps too, which would correspond to the deposition of a rectangle or correlated deposition of squares.

In our simulations we measured the time dependence of the average surface width

$$w^2(t)=\langle[h(i,t)-\overline{h(t)}]^2\rangle_i, \tag{5}$$

where $h(i,t)$ is the height at site i, $\langle\ \rangle_i$ means averaging over the sites, and $\overline{h(t)}$ is the average height function

$$\overline{h}=\langle h(i,t)\rangle_i.$$

In a broad class of growth models $w(t)$ behaves according to the KPZ theory [13], that is,

$$w\sim t^{\beta} \quad \text{if } t\ll L^z \tag{6}$$

and

$$w\sim L^{\alpha} \quad \text{if } t\gg L^z. \tag{7}$$

TABLE III. Simulations performed for the measurement of $w^2(t)$ for $v_{\max}=1$.

System size L	Number of runs
1024	500
2048	200
4096	50

The simple deposition model corresponding to the $v_{\max}=1$ case is known to belong to this universality class [12].

As an initial condition we used equally distributed cars. For the uniformly distributed initial condition we received large fluctuations and have not seen any regularity. In that case we saw the same behavior as in the system with an equally distributed initial condition after relaxation. We subtracted the average steepness from the surface height in order to calculate $w^2(t)$. The simulations performed are listed in Tables III and IV.

In the $v_{\max}=1$ case in the whole density region we see KPZ-like behavior (Fig. 7) and we obtain $2\beta=0.63\pm0.04$ and $2\alpha=0.99\pm0.06$, which should be compared to the KPZ values $\beta=\frac{1}{3}$ and $\alpha=\frac{1}{2}$. This KPZ-like behavior explains the value of the x exponent close to $\frac{2}{3}$ obtained from the relaxation time analysis (4) because the velocity of the cars

$$\overline{v}(t+1)=\frac{1}{2}\sum_{i=1}^{L}[h(i,t+1)-h(i,t)]=\frac{L}{2}[\overline{h}(t+1)-\overline{h}(t)], \tag{8}$$

that is,

$$\frac{2}{L}\overline{v}(t)=\frac{d\overline{h}}{dt}\equiv v_s(L,t). \tag{9}$$

According to [14],

$$\Delta v_s(L,t)=v_s(L,t)-v_s^0\sim t^{-\alpha_\perp} \quad \text{for } t\ll L^z, \tag{10}$$

where v_s^0 is $v_s(L,t)$ for $t,L\to\infty$. The exponent $\alpha_\perp$ corresponds to our x exponent and is in one dimension $x=\alpha_\perp=\frac{2}{3}$.

In the $v_{\max}=2$ case the shape of the $w^2(t)$ curves is also KPZ-like. We measured 2α to be $2\alpha=1\pm0.05$. In contrast to the $v_{\max}=1$ case, the β exponent depends on the density, as seen in Fig. 8, and it is not uniform as in the $v_{\max}=1$ case.

V. CORRELATION FUNCTIONS

Finally, we studied the velocity correlation function in the space of car series with the definition

TABLE IV. Simulations performed for the measurement of $w^2(t)$ for $v_{\max}=2$.

System size L	Number of runs
512	20 000
1024	10 000
2048	5000

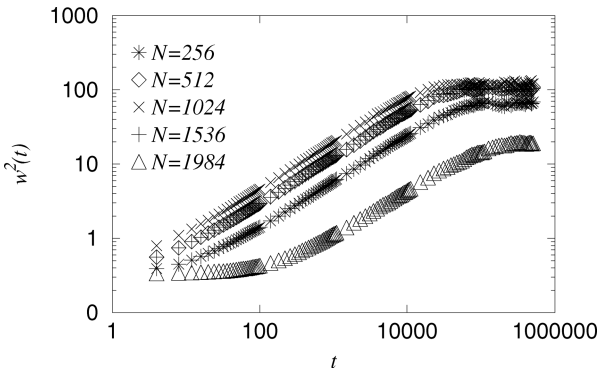

FIG. 7. Square of the average surface widths versus time graph for the $v_{\max}=1$ case for different densities. The system size is $L=2048$ and the curves correspond to the densities $\rho=0.125$ ($N=256$), $\rho=0.25$ ($N=512$), $\rho=0.5$ ($N=1024$), $\rho=0.75$ ($N=1536$), and $\rho=0.968\,75$ ($N=1984$). On the log-log plot the KPZ-like behavior is apparent.

$$C(i,t)=\langle[v(j,t')-\overline{v(t')}][v(j+i,t'+t)-\overline{v(t'+t)}]\rangle_j \tag{11}$$

or

$$C'(i,t)=\langle v(j,t')v(j+i,t'+t)\rangle_j, \tag{12}$$

where $v(j,t)$ is the velocity of the jth car at time t, $\langle\ \rangle_j$ means averaging over all cars, and t' is a time when the system is in the steady state. Since $C(i,t)$ is in the stationary state it is independent of t'.

If we consider the function $C(i,t)$ at a constant time t as a function of i, we find a peak centered at the value

$$i(t)=\max_j C(j,t). \tag{13}$$

The maximum of the peak decreases with increasing t (Fig. 9). $i(0)=0$ because that is the autocorrelation function, but for greater times it appears at other car indices. Considering the $i(t)$ versus t graph, we can fit on the $i(t)$ values a straight line whose steepness depends on the density. This steepness defines a velocity in the car series space with which the peak spreads. Except for the peak, the $C(i,t)$ function fluctuates around a constant value and it forms a plateau.

From the definition of $C(i,t)$ it follows that the jammed cars do not contribute to $C(i,t)$ since they are staying. The

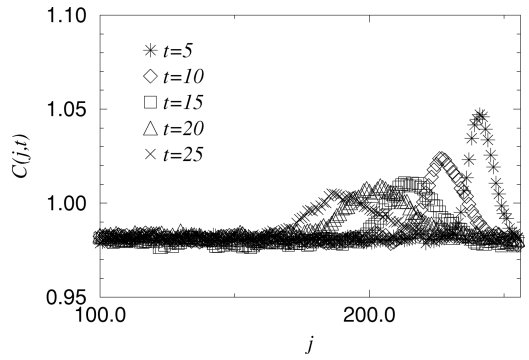

FIG. 9. Correlation times versus car index for different times. The parameters of the system are $L=256$, $\rho=0.5$, and $v_{\max}=2$.

cars already accelerated near $v_{\max}$ contribute to the plateau of $C(i,t)$. Those cars contribute to the peak which accelerate in a correlated manner because a car accelerating makes space for the car behind to accelerate. These are the cars coming out of a jam. Therefore, the long-term existence of the peak and its velocity characterizes the traffic jams in the system.

In the $v_{\max}=1$ case the $V_1(\rho)$ velocity of the peak increases without any sign of criticality from zero to its value at $\rho=1$, where $v(\rho\to1)=1-p$. This value follows from the motion of a single hole (Fig. 10).

However, in the $v_{\max}=2$ case we can see a bending at the $V_2(\rho)$ function at the density $\rho_k=0.125$ where the function shows a steep increase (Fig. 11). This implies emerging traffic jams. The small $V_2(\rho)$ values of the function below ρ_k come from the small fugitive jams being in the system. It is tempting to interpret the bending in $V_2(\rho)$ as the appearance of a new phase at ρ_k, since the behavior of the peak velocity is reminiscent to an order parameter of second order phase transitions. However, the velocity does not go to zero at the bending point and—in contrast to what is expected for second order transitions—we could not observe any finite size scaling.

VI. THE $V_{\max}=\infty$ CASE

Our simulations have indicated the following. (i) The behavior $v_{\max}>1$ is different from $v_{\max}=1$. (ii) For $v_{\max}>1$ there is a jamming transition, but a careful study of the different characteristics indicated, in contrast to what was suggested in [10], that there is no clear second-order phase tran-

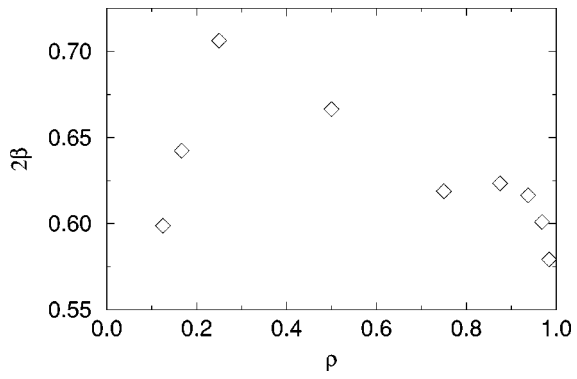

FIG. 8. 2β exponent measured in the $v_{\max}=2$ model for different densities.

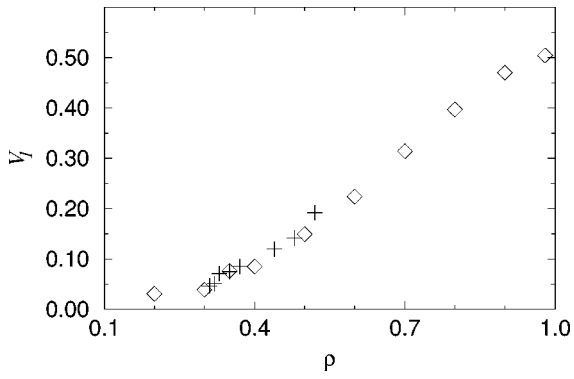

FIG. 10. Peak velocity $V_1(\rho)$ as a function of the density for $v_{\max}=1$.

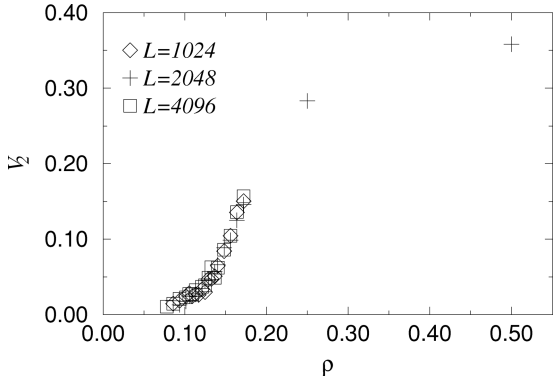

FIG. 11. Peak velocity $V_2(\rho)$ as a function of the density for $v_{\max}=2$.

sition related to it. (iii) From the present and earlier studies [7,10,15] it is clear that the smaller p is the more pronounced the transition. (iv) Comparing our results for $v_{\max}=2$ with those for $v_{\max}=5$, we realize that increasing $v_{\max}$ also sharpens the transition.

The origin of (iii) is clear: In the $p=0$ model there is a phase transition related to a singularity in the fundamental diagram. In order to see the origin of (iv) we considered the case without a speed limit, more precisely, the $v_{\max}=L$ case.

The fundamental diagram of the $v_{\max}=\infty$ case shows different features from the cases discussed so far (Fig. 12). The main characteristic of its shape is a plateau value depending on p (Fig. 13). The function decreases quickly to this plateau. The height of the plateau is independent of the system size; only its length changes.

Looking at the flow of the cars, we can observe that at the densities where the current of the stationary state $j_\infty(\rho)$ is higher than the j_p plateau value the cars tend to be equally distributed, which is typical for the deterministic case [6]. However, at the density regime of the plateau we see one jam, which characterizes this density region (Fig. 14). For higher densities where $j_\infty(\rho)$ decreases with the density we see more than one jam. Calculating the correlation function (12) we notice that the $v_\infty(\rho)$ peak velocity in the plateau region corresponds to j_p, which also means that we have only one jam in the system for these densities.

Assuming that the ρ_t value where the plateau sets in depends on L, like

$$\rho_t \sim L^{-t}, \tag{14}$$

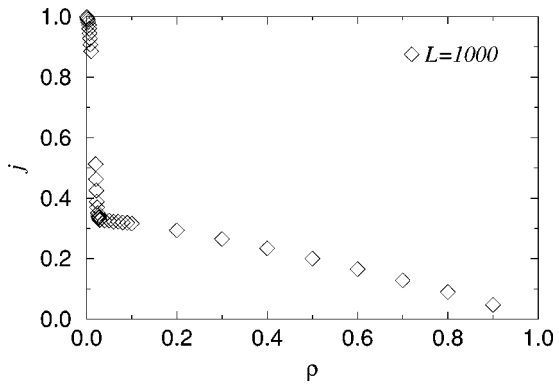

FIG. 12. Fundamental diagram for $v_{\max}=\infty$ for $L=1000$.

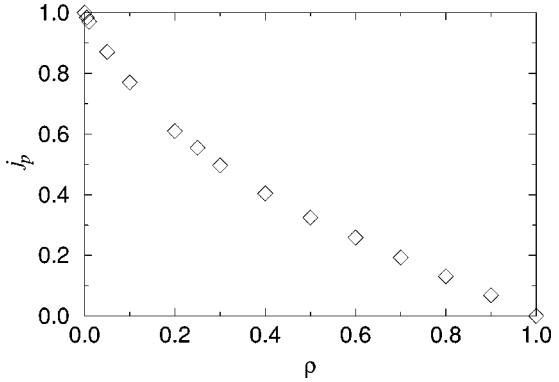

FIG. 13. Plateau values for different p braking probabilities in the $v_{\max}>\infty$ model.

we obtain $t\approx 0.5$. Because this point represents the $N_f=\rho_t L$ number of cars being in the flow between the right- and left-hand sides of the jam, we can conclude that the density contribution of cars in the flow part scales as

$$\rho_f \sim L^{-t} \tag{15}$$

and therefore the density contribution of the cars being in the jam will be

$$\rho_j = \rho - \rho_f, \tag{16}$$

$$\rho_j \to \rho \quad \text{when} \quad L \to \infty. \tag{17}$$

Thus values greater than the j_p plateau value of $j_\infty(\rho)$ (except the value at $\rho=0$) can be considered as fluctuation effects. When $\rho \to 0$ we have a finite number of cars with an infinite velocity (one car with velocity $L-1$). In the thermodynamic limit

$$j_\infty(\rho \to 0) = \frac{L-1}{L} \quad \text{as} \quad L \to \infty. \tag{18}$$

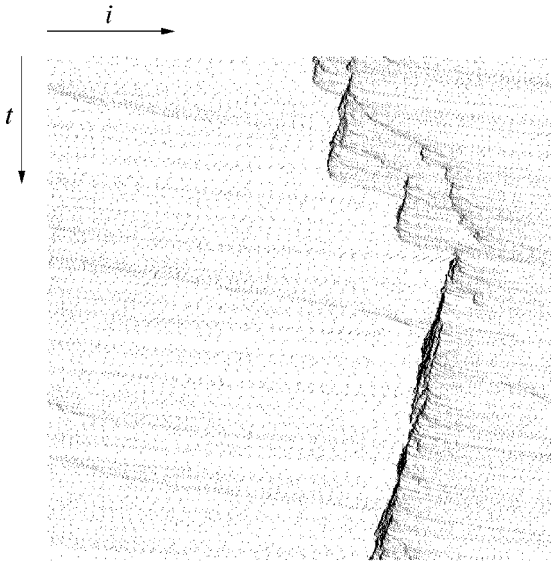

FIG. 14. One-jam phase of the $v_{\max}>\infty$ model. The horizontal direction represents the lattice sites and the vertical direction the consecutive time steps.

Therefore, we can say that in the thermodynamic limit we have a phase transition at $\rho=0$ between the phases of $j_\infty(0)=1$ and no jams and of the j_p value with one jam. Increasing ρ, the plateau ceases and there is more than one jam in the system. This result contradicts that of the mean-field theory described in [6], where the fundamental diagram starts at the $\rho=0$, $j=0$ point with infinite slope. For braking probabilities smaller than $p=0.001$ the plateau ceases and only a break in the graph remains.

VII. CONCLUSION

According to our comparison of the three different models we can conclude the following. As we summarized at the beginning of Sec. VI, there is a difference between the behavior of the $v_{\max}=1$ and $v_{\max}>1$ models. In contrast with the $v_{\max}=1$ model, in the $v_{\max}=2$ case we see a transition but it is not a strict second-order transition; it seems to be a crossover transition. We found that the density at which the transition takes place is smaller than the $\rho_c=0.19$ value mentioned in [16]. On the grounds of the results obtained for $v_{\max}=\infty$, where we found a first-order transition, we can conclude that the increase of the $v_{\max}$ parameter makes the transition more striking. Our results indicate that the behavior of the models labeled by different p and $v_{\max}$ parameters is guided by the transition points of the models with parameters $p=0$ or $v_{\max}=\infty$.

ACKNOWLEDGMENT

This work was supported by OTKA T016568.

[1] I. Prigogine, in *Theory of Traffic Flow*, edited by R. Herman (Elsevier, Amsterdam, 1961), pp. 158–164.
[2] *Traffic and Granular Flow*, edited by D. E. Wolf, M. Schreckenberg, and A. Bachem (World Scientific, Singapore, 1995).
[3] K. Nagel and M. Schreckenberg, J. Phys. I **2**, 2221 (1992).
[4] Z. Csahók and T. Vicsek, J. Phys. A **27**, L591 (1994).
[5] T. Nagatani, J. Phys. A **51**, 922 (1995).
[6] M. Schreckenberg, A. Schadschneider, K. Nagel, and N. Ito, Phys. Rev. E **51**, 2939 (1995).
[7] K. Nagel and M. Paczuski, Phys. Rev. E **51**, 2909 (1995).
[8] M. Leibig, Phys. Rev. E **49**, 184 (1994).
[9] K. Nagel and S. Rasmussen, in *Proceedings of the Fourth International Workshop on the Synthesis and Simulation of Living Systems*, edited by R. A. Brooks and P. Maes (MIT Press, Cambridge, MA, 1994), pp. 222–235.
[10] G. Csányi and J. Kertész, J. Phys. A **28**, 427 (1995).
[11] L. C. Q. Vilar and A. M. C. de Souza, Physica A **211**, 84 (1994).
[12] P. Meakin, P. Ramanal, L. M. Sauder, and R. C. Ball, Phys. Rev. A **34**, 5091 (1986).
[13] A.-L. Barabási and H. E. Stanley, *Fractal Concepts in Surface Growth* (Cambridge University Press, Cambridge, 1995).
[14] J. Krug and P. Meakin, J. Phys. A **23**, L987 (1990).
[15] K. Nagel and H. J. Herrmann, Physica A **199**, 254 (1993).
[16] A. Schadschneider and M. Schreckenberg, J. Phys. A **30**, L69 (1997).